Quarterly Progress Report - 13 August to
13 November 1965

HIGH-PERFORMANCE THERMIONIC CONVERTER

Prepared for
Jet Propulsion Laboratory
California Institute of Technology
4800 Oak Grove Drive
Pasadena, California
Attention: Mr. Jack L. Flatley, Contract Negotiator

Contract 951225

EOS Report 6952-Q-2 23 December 1965

Prepared by
A. E. Campbell
D. H. Pollock

Approved by
A. O. Jensen, Manager
SPECIAL TUBE DEPARTMENT

Approved by
George R. White, Manager
OPTICAL ELECTRONICS DIVISION

This work was performed for the Jet Propulsion Laboratory, California Institute of Technology, sponsored by the National Aeronautics and Space Administration under Contract NAS7-100.

ELECTRO-OPTICAL SYSTEMS, INC. — PASADENA, CALIFORNIA
A Subsidiary of Xerox Corporation

CONTENTS

CONTENTS (contd)

ILLUSTRATIONS

ILLUSTRATIONS (contd)

1. INTRODUCTION

This is the second quarterly report of progress on JPL Contract 951225, a program to (1) investigate basic materials, processes, and operating parameters affecting the stability and optimization of cesium-vapor thermionic converters, and (2) apply the results of these investigations to the fabrication of practical, high-performance, high-efficiency, long-life cesium-vapor thermionic converters.

1.1 Program Goals

The program goals are: (1) to generate fundamental data on the various converter operational parameters such as interelectrode spacing, Langmuir-Taylor type cesiated electron emission and work function of various electrode materials, and to establish optimum electrode materials processing, all to be applicable to practical cesium-vapor thermionic converters; (2) to conduct auxiliary experiments pertinent to the engineering design and converter fabrication in a manner such that the results are applicable to practical, high-efficiency, long-life cesium-vapor thermionic converters, and (3) to design, fabricate, and test a maximum of six cesium-vapor thermionic converters utilizing the results of the auxiliary experiments, leading to a performance of 20 watts/cm^2 at 0.8 volt output and an efficiency exceeding 14 percent for an emitter temperature of 1735°C.

Adequate attention will be accorded the collector and radiator heat-transfer problems so that a converter with a 2-cm^2 emitter having an output of 40 watts at 0.8 volt can be fabricated with a minimum radiator weight. The weight of the converters must be consistent with the achievement of a four-converter generator weighing less than 4 pounds. The radiator area of the converters must be such that no additional cooling (such as excessive thermal conduction down the collector lead straps) is necessary for operation of the converter at its design conditions.

1.2 Summary of Work Performed During Reporting Period

The variable-parameter test vehicle was completely fabricated, loaded with cesium, instrumented for performance testing, and is currently being used to gather optimization data. All auxiliary apparatus, such as the drive mechanism and the constant voltage-constant current load, were assembled, pretested, and integrated into the test vehicle system.

Three outgassing schedules for rhenium emitters were examined for grain growth stability. The third emitter is still undergoing investigation.

A thermal mockup of a molybdenum collector-copper radiator was fabricated and tested for reliable heat transfer and increased heat rejection/unit weight.

Three high-alumina, ceramic-to-metal seal assemblies were fabricated and tested for resistance to repeated thermal shock.

A comparative examination of reservoir pinch-offs was conducted to select a pinch-off tool and processing schedule which would result in a highly reliable (maximum sealing area) pinch-off.

A number of electron-beam weld samples (rhenium) were metallurgically examined for penetration characteristics. The results of this examination were applied to the successful electron-beam welding of the test vehicle.

A design analysis for converter SN-101 has been completed. It includes the following:

1. The choice of electrode materials
2. A computed converter efficiency for operation at the design point of 20 watts/cm^2 at 0.8 volt
3. The collector heat load and subsequent radiator geometry
4. An assembly procedure for the final step in fabrication, which involves the electron-beam welding of prefabricated seal assemblies to the converter structure

1.3 Summary of Significant Results and Conclusions

A preliminary test of the drive mechanism demonstrated that interelectrode spacings in the test vehicle can be established within 0.0001 inch.

The test vehicle return drive rods, springs, and 0.0001-inch indicators were operated under thermal loads approximating test vehicle operation. Temperature measurements on the indicators were on the order of 30°C.

An outgassing schedule for rhenium and tantalum emitters has been established which results in emitting surfaces that indicate only minimal grain growth after 100 hours operation at 2000°K.

A molybdenum collector-copper radiator assembly has been fabricated and tested with the following results:

1. The braze-joint geometry retained mechanical strength and integral bonding over 300 thermal shock cycles while transferring 200-225 watts (thermal).
2. The assembly weighs approximately the same as the EOS all-molybdenum forging, yet it rejects almost twice as much heat.
3. No shaling or peeling of Rokide "C" from the copper radiating fin occurred during thermal-cycle testing at 600°C.

The active alloy (Ni-Zr) brazing of high-purity alumina to niobium has remained leak tight through thermal shock cycles at a heating rate of 100°C/min. These seals also have operated at 700°C for 500 hours and remained leak tight. The ease of fabrication and the ability of pretesting metal-ceramic seal subassemblies has provided a significant advance for converter fabrication.

2. ELECTRODE MATERIALS EVALUATION

2.1 Variable-Parameter Test Vehicle

During the second quarter of effort, the variable-parameter test vehicle components were fabricated and the vehicle assembled. Experiments were conducted to determine the thermal environment to which the spacing dial indicators would be subjected. The sheathed thermocouples immersed in the collector barrel have been brazed into position and calibrated *in situ*. Sample bellows were fabricated and cycle tested and the excursion forces were measured. The electronic load has been tested and incorporated into the test apparatus.

2.1.1 Vehicle Fabrication

2.1.1.1 Vehicle Assembly

As a result of the electrode materials design review meeting with JPL, the first combination of materials selected for study was a rhenium emitter and a rhenium collector.

A view of the disassembled variable-parameter test vehicle is shown in Fig. 2-1. The rhenium heat choke envelope was joined to the molybdenum emitter plate by a titanium braze (1668°C). The titanium braze was chosen rather than a vanadium braze due to the high temperature required for the latter (1900°C). Sample brazes indicated the possibility of introducing stress cracks in the molybdenum at this temperature. This is caused by a combination of factors, including the machined geometry of the braze grooves in the molybdenum and the differential expansions of the various materials involved. The titanium braze was completed successfully.

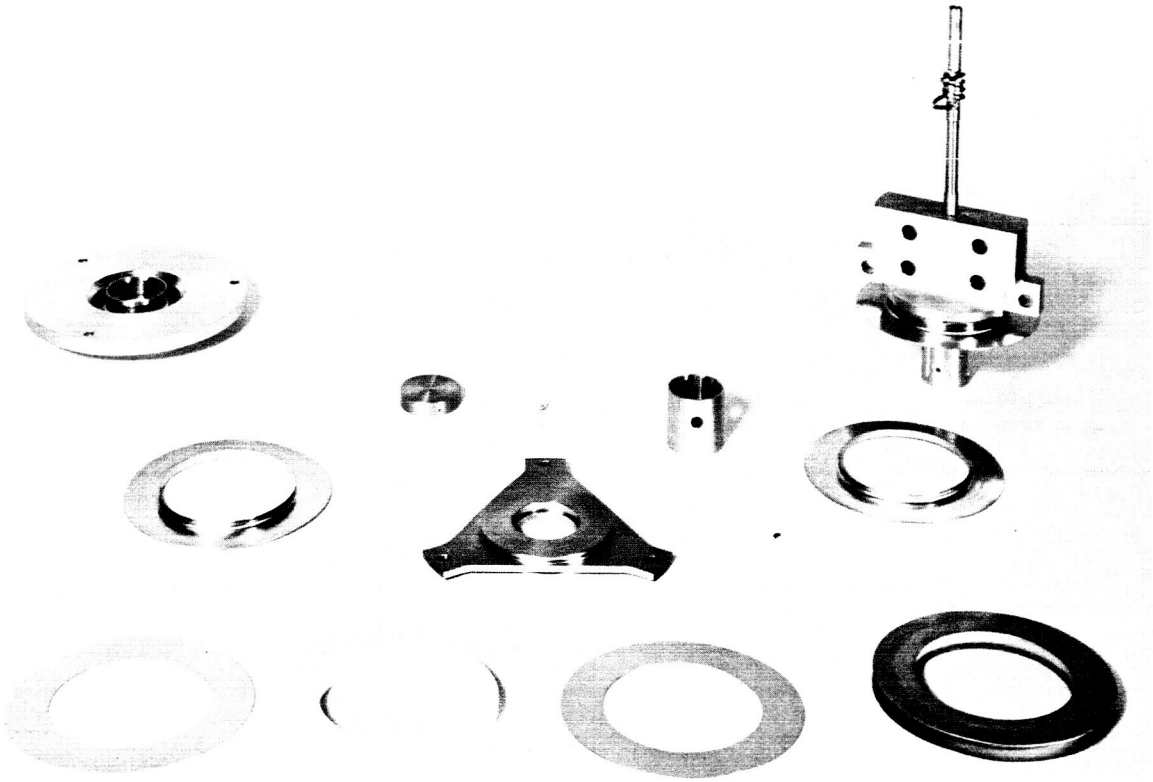

FIG. 2-1 VARIABLE-PARAMETER TEST VEHICLE COMPONENTS AND SUBASSEMBLIES

The guard ring subassembly fabrication procedure consists of brazing the guard ring barrel to the guard ring lead plate and joining two niobium bellows flanges to the top and bottom of the lead plate. All of these joints were brazed simultaneously using a titanium braze.

The collector subassembly is comprised of a rhenium shim brazed to the surface of the molybdenum collector-radiator, a niobium collector flange, and a tantalum-cesium reservoir tubulation. The rhenium shim was vanadium brazed to the molybdenum collector in a rough-machined condition. After the braze, the collector and shim were finished-machined to the appropriate dimension. At this point, the niobium flange and tantalum reservoir were titanium brazed to the collector-radiator. After the titanium braze, the rhenium collector surface was faced to remove any condensed braze material. Finally, the sheathed thermocouples were inserted into the collector barrel with thin (0.001-inch) copper foil wrapped around the end of the thermocouple. The collector-radiator was raised to a temperature of 1100°C to effect a copper braze.

Four ceramic-metal seal subassemblies were fabricated by joining high-purity alumina ceramics (AL 995 Wesgo) to flat niobium flanges. These are to be included into the bellows-seal assembly. The metal-ceramic seals were effected by the EOS standard, active-alloy braze (GMP 34200/020).

After the brazed assemblies are complete, they are stacked on the vehicle and joined by welding at the bellows seals. Both electron-beam and tungsten-inert gas welding methods were utilized to complete feasibility bellows. The electron-beam welding method was adopted because it provides greater control of power input to the flanges.

When the bellows seals are completed, the vehicle is placed in a jig which can expand the bellows by 0.005 to

0.008 inch. The rhenium emitter is then inserted into the rhenium heat choke envelope and electron-beam welded into position. The emitter is purposely allowed to be in physical contact with the collector surface (with expanded bellows) for the beam weld in order to achieve controlled shorting of the emitter and collector at high emitter temperatures during test.

2.1.1.2 Vehicle Support Fixtures

The completed vehicle testing layout is shown in Fig. 2-2. Shown in the figure are the gantry, drive mechanism, return rods, spacing indicators, lead straps, and cooling rings. Figure 2-3 is a top view of the drive mechanism control showing the gear train, gauged gear drive and individual rod drives.

2.1.2 Associated Vehicle Experiments

2.1.2.1 Dial Indicators

An experiment was conducted to determine whether there were any thermal effects on the dial indicators when operated within the vacuum test station under conditions to be encountered during vehicle test. The steady-state operating temperature of the dial indicators also was determined. A heated, molybdenum test-vehicle mockup was supported by the drive and measuring chain. Ten, dimpled layers of 0.001-inch molybdenum sheet were placed on top of the bottom plate of the gantry. The dial indicators were placed in position. One indicator was wrapped in nickel foil to shield it from thermal radiation while another indicator was left bare. Thermocouples were placed on the molybdenum plate, on the bottom of the gantry plate, and on the dial indicators. The results of the test show that, with the molybdenum test vehicle mockup held at an equilibrium temperature of 630°C for over 3 hours, the bottom of the gantry plate reached an equilibrium temperature of 39°C, the shielded indicator reached an equilibrium temperature of 34°C, and the unshielded indicator reached a temperature of 25°C. Thus, it may be

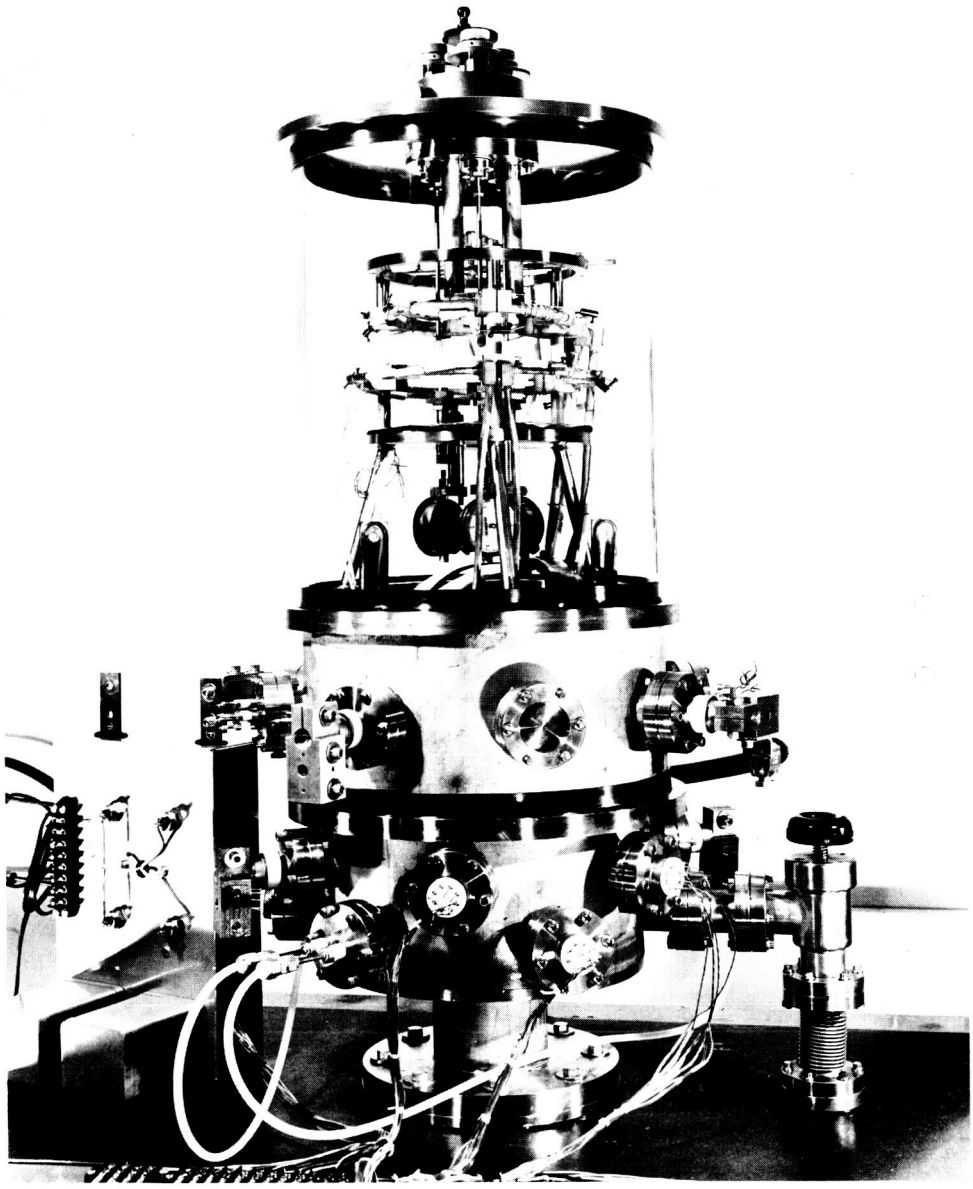

FIG. 2-2 TEST VEHICLE DRIVE MECHANISM, TEST CIRCUITRY, AND INSTRUMENTED VACUUM CHAMBER

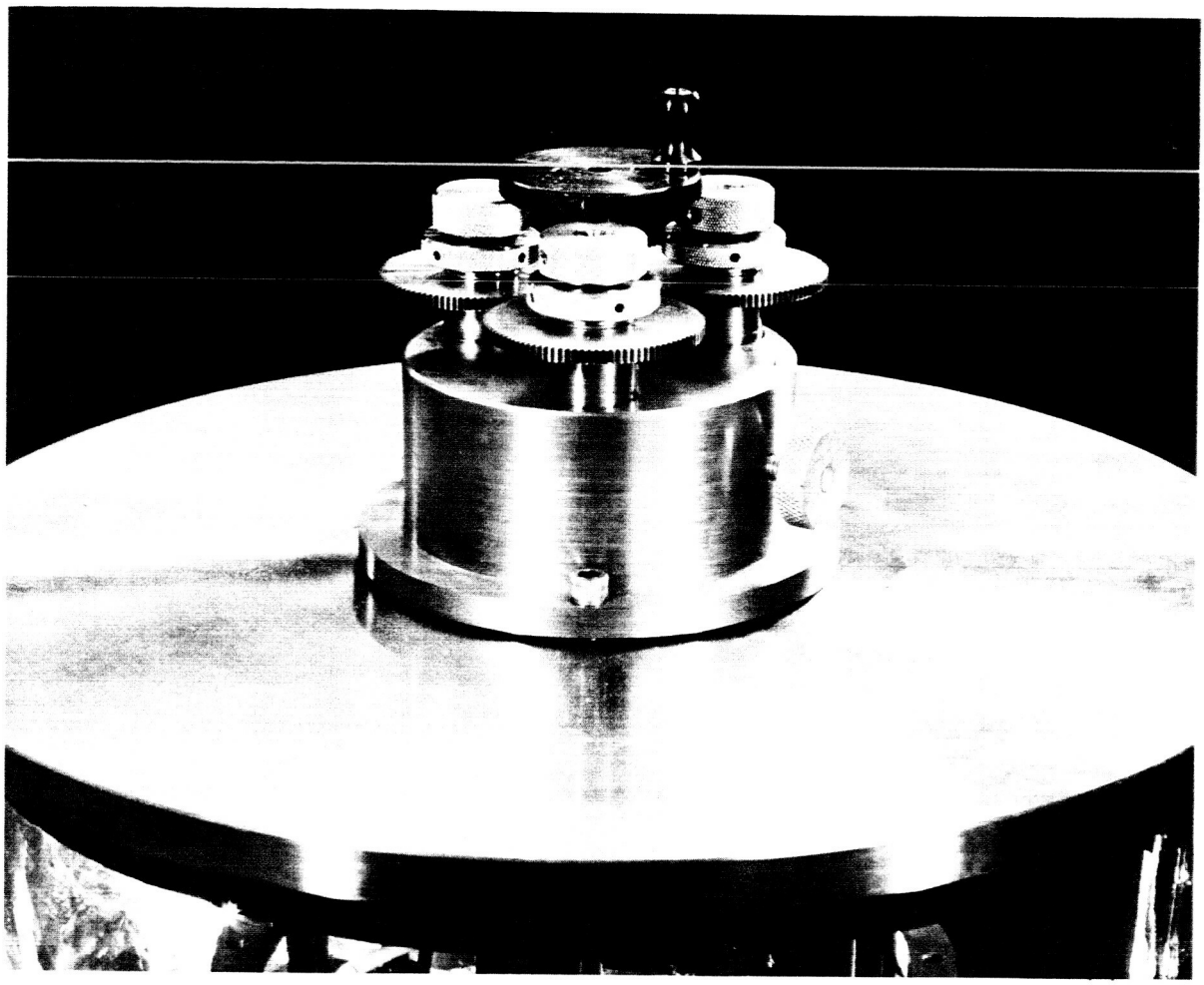

FIG. 2-3 TEST VEHICLE DRIVE MECHANISM

concluded that the major source of heat input to the dial indicators is conduction down the support linkage. The heat shielding of the gantry plate was adequate for maintaining a 600°C temperature difference between the simulated test vehicle and the gantry parts. If a temperature of 30 to 40°C is maintained at the dial indicators during actual vehicle testing, there should be no problem of maintaining dial indicator accuracy.

2.1.2.2 Bellows Experiments

A sample ceramic-bellows seal subassembly was tungsten-inert gas welded. The flange dimensions were identical to those of the variable-parameter vehicle, 2.400 inches in diameter. The flange material is niobium. A stainless steel ring 0.100 inch thick and having an outside diameter of 1.925 inches, was used in place of an alumina ceramic. The stainless steel ring was spot welded between two flat niobium flanges similar to an actual ceramic seal assembly. Copper split rings with an inside diameter slightly larger than the OD of the ceramics and an outside diameter 0.020 inch less than the OD of the niobium flanges was inserted between the two weld zones and above and below the welds. The whole assembly was clamped tightly to produce an excellent heat transfer path for the thermal input resulting from the welding process.

Immediately after welding, an excursion force of 0.432 lb/mil over a 0.025-inch excursion was measured with the bellows in the unannealed state. The bellows was then placed on life cycle test. After experiencing over 2000 cycles of 0.025-inch travel without any outward signs of fatigue, the excursion was measured and found to be 0.54 lb/mil. This increase in excursion force is due to work hardening of the bellows material.

As stated in the first quarterly report (EOS Report 6952-Q-1), the force needed to open the bellows 0.025 inch during

test will be derived from the spring-loaded return rod assembly beneath the emitter plate. The drive rods from above will be utilized only to close the spacing between the emitter and collector. A test was made to determine the amount of return rod spring compression required to provide the proper excursion force measured from the sample test bellows. The three return rod springs were mounted on a plate in their unloaded condition. A plate was placed on top with a pressure of 10.8 lbs (the force required to extend the bellows 0.025 inch) and the springs compressed 0.132 inch. Thus, compressing the springs this amount in the gantry will produce the force required to open the interelectrode spacing of the variable-parameter vehicle by 0.025 inch.

2.1.2.3 Collector Thermocouples

As discussed above, two tantalum-sheathed thermocouples, 6 inches long and 0.040 inch in diameter, using a 0.005-inch-diameter platinum wire and a 0.005-inch-diameter 90-percent platinum 10-percent rhodium wire, were brazed into the collector subassembly. In order to calibrate the immersion thermocouples after brazing the following procedure was employed:

The collector subassembly was installed in a 400 liter/sec ion-pumped vacuum station. To minimize heat conduction losses, the collector was mounted on ceramic insulators. Secondary standard chromel-alumel thermocouples were placed around the collector barrel at heights corresponding to the heights of the immersed thermocouples. A refractory oven was placed over the collector barrel assembly. The complete test arrangement is shown in Fig. 2-4. During the calibration run, only small temperature differences of approximately $3^{\circ}C$ were observed between the two sheath thermocouples. This indicates the collector barrel had no significant temperature drop down the barrel. This is reasonable since the heat lost by radiation was no greater than 4 watts at $500^{\circ}C$ for a radiating area of 20 cm^2. Figure 2-5 shows the actual thermocouple calibration. The data recorded were obtained as the collector assembly cooled down with oven power off. This eliminated radiation heating of the standard thermocouples mounted on the outside diameter of the collector barrel.

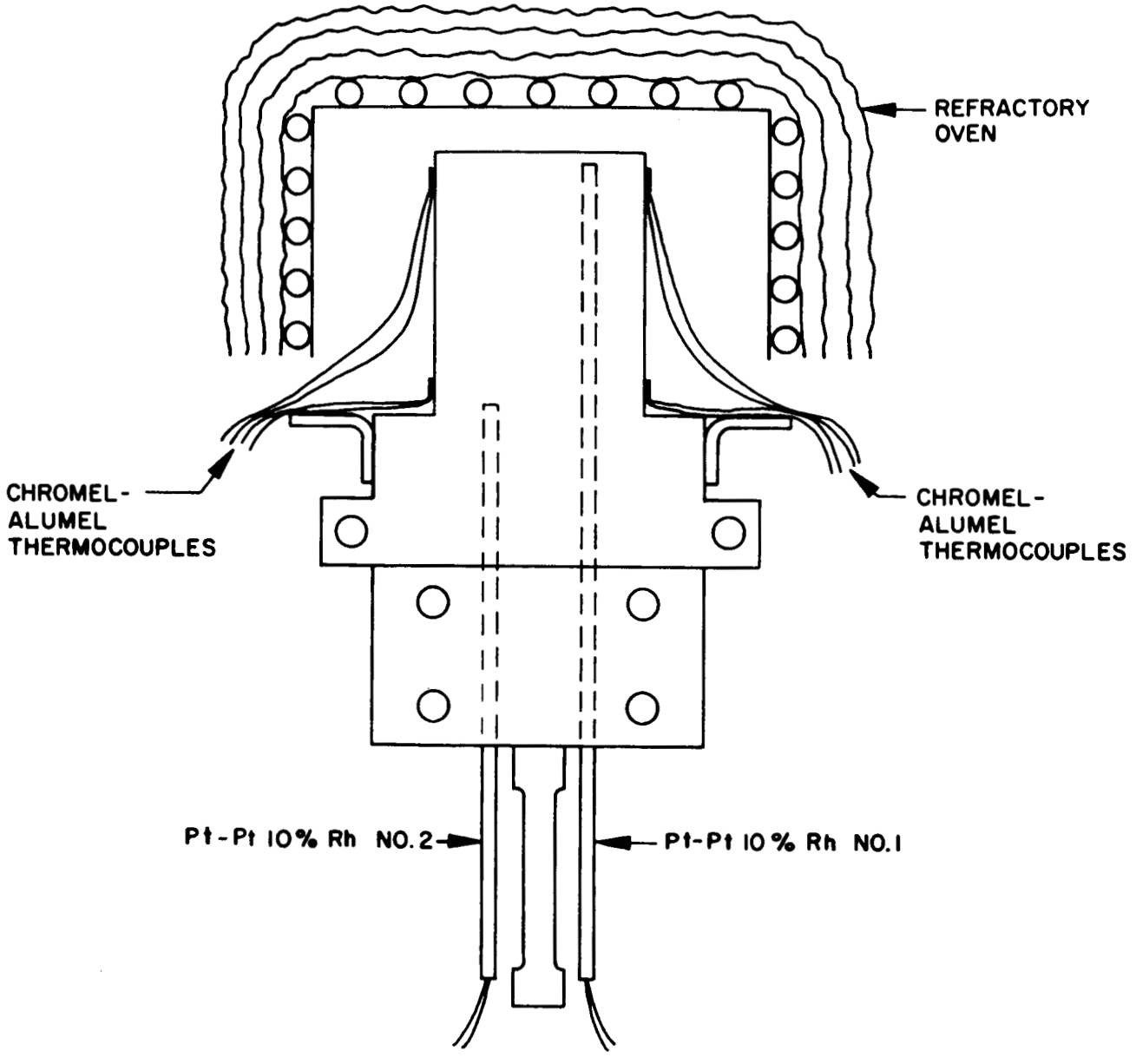

FIG. 2-4 TEST VEHICLE COLLECTOR THERMOCOUPLE CALIBRATION SETUP

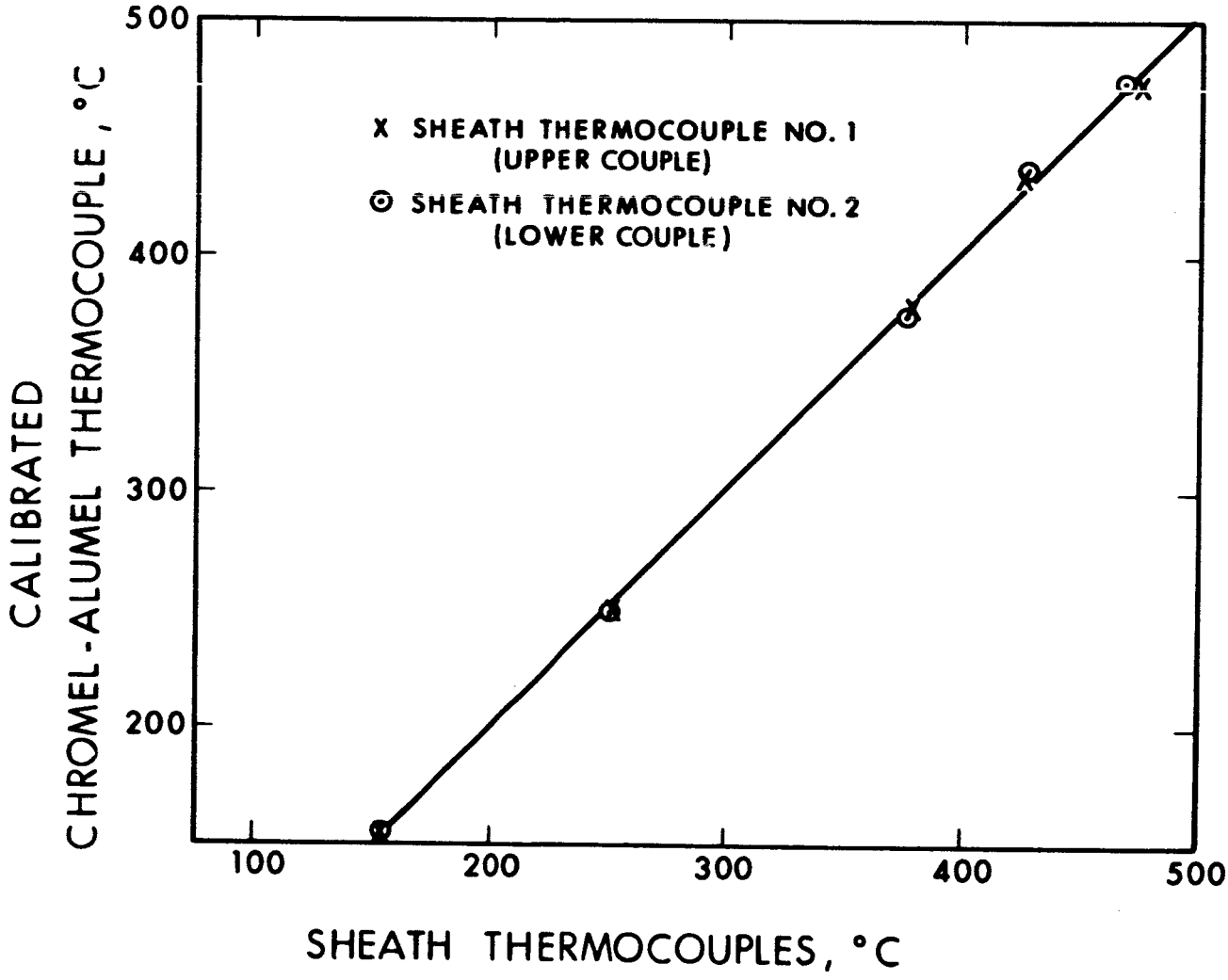

FIG. 2-5 TEST VEHICLE COLLECTOR THERMOCOUPLE CALIBRATION

2.1.3 Test Circuitry

Figure 2-6 is a performance plot of the regulating ability of the test vehicle electronic load. The plot of these data was set up to easily show the variations in voltage about a given set point. On the figure, the circled numbers on the y-axis represent the selected set points. The ±0.5 above and below the set points are millivolt deviations from the set point as read on a digital voltmeter. An arbitrary current of 50 amperes was selected as a reference starting point. As the current through the load was varied, the deviation from the set point was recorded and plotted.

The asymmetry of the curves is due to the input characteristics of the voltage comparator transistor (input transistor 2N43A). This expected effect results from the change in voltage that is dropped across this transistor with changes in current through the transistor base. The voltage drop in the base circuit also is the factor which limits the minimum operating voltage of the load to 0.2 volts. This voltage drop is an inherent characteristic of any transistor.

The vehicle test circuit is shown in Fig. 2-7. The important features of this testing circuit are the constant load discussed above and the equalizing resistor shown in Fig. 2-7. This resistor will be used to null the current between the guard ring and collector circuits to accurately define the measured current density.

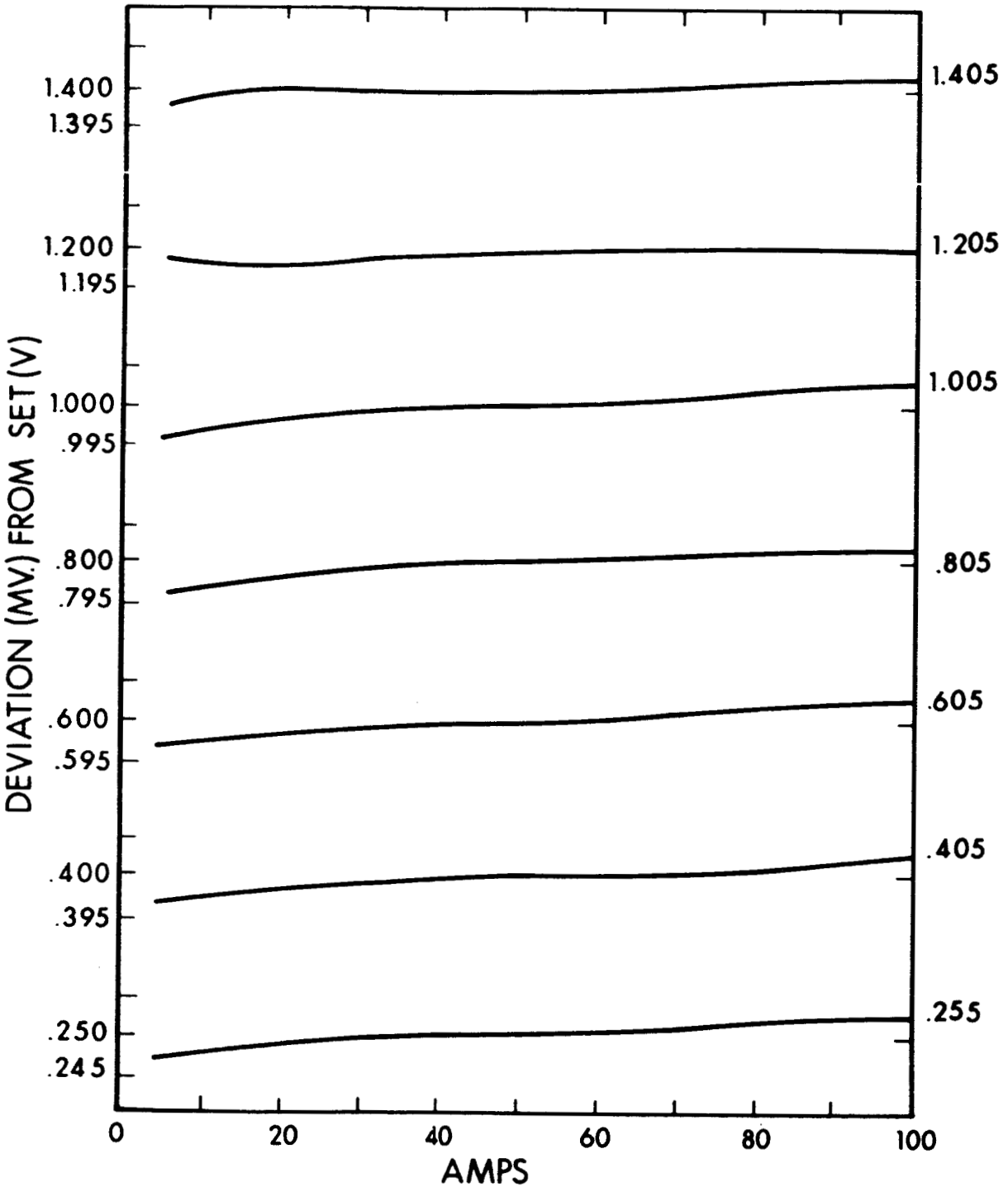

FIG. 2-6 ELECTRONIC LOAD PERFORMANCE CURVES

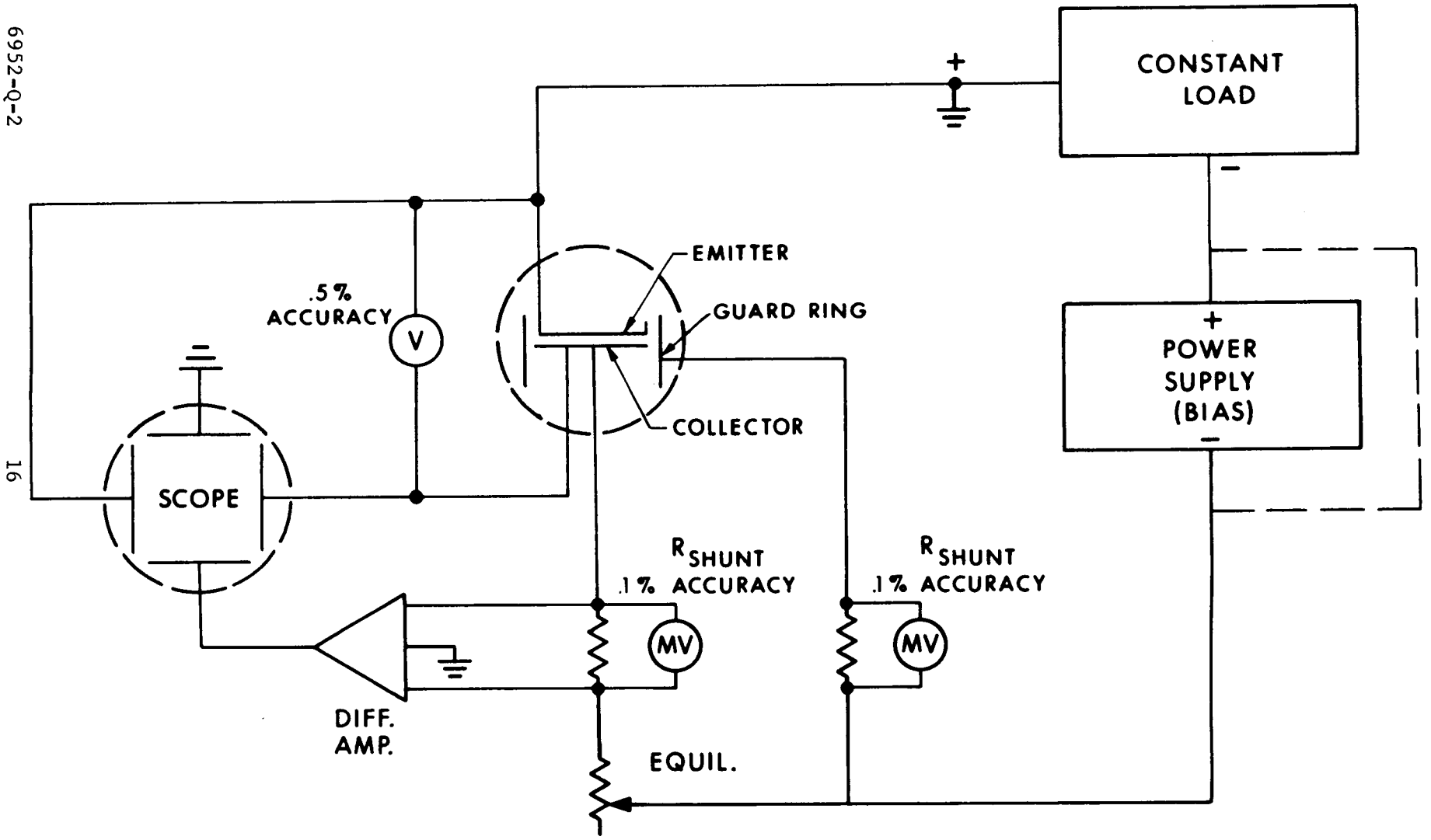

FIG. 2-7 SCHEMATIC OF TEST VEHICLE CIRCUITRY

2.2 Emitter Materials Process Study

The emitting electrode in the EOS high-performance thermionic converter operates at a specified design temperature of 2000°K. Operation at these temperatures may result in excessive grain growth and variable average emission if the emitter surface has not been previously heat-treated sufficiently to establish a stable grain structure. Since all material intended for electrode use in a thermionic converter is vacuum heat-treated or outgassed, the problem becomes one of determining an outgas schedule which will not only remove gaseous impurities and high-vapor-pressure elements, but will establish a stable surface for subsequent long-term operation in a converter.

The objective of this study is to generate a processing schedule for the emitter materials of tantalum and rhenium. The previous quarterly report of progress on this program (EOS Report 6952-Q-1) contained the detailed procedures for machining and cleaning tantalum. Outgassing schedules of 2100°C and 2250°C for 2 hours each were found to yield tantalum emitter surfaces whose grain structure had been radically altered during 100-hour operation at 1735°C. A final sample was outgassed at 2450°C for 2 hours. This schedule produced a surface which exhibited only minor changes as a result of 100 hours operation at 1735°C.

2.2.1 Preparation of Rhenium Samples

Three plate-stock rhenium disks of 0.800-inch diameter and 0.200-inch thickness were ground to achieve flatness and perpendicularity to 0.0001-inch tolerance. Such tolerances are necessary for accurate measurements of thermionic power output from the variable-parameter vehicle at small (0.001-inch) interelectrode spacings. Measured tolerances on an electronic micrometer were less than 10 millionths of an inch, the limit of the measuring instrument. The grinding operation, performed with fine-grit diamond wheels, was

followed by diamond-dust lapping and polishing to achieve final surface smoothness. Profilometer readings indicated a surface smoothness of less than 10 microinches.

Grinding and polishing are acceptable techniques of working rhenium since the material is not amenable to standard shop practices of facing and turning. Rhenium work-hardens so easily that neither fully treated tool steel nor cemented tungsten carbide is capable of taking accurate cuts of the material. In addition, rhenium does not pick up polishing or lapping compounds as does tantalum, hence, it remains free of contaminants from these polishing operations. Pyrometer sight holes having 8:1 depth-to-diameter ratios are electric-discharge machined in ethyl alcohol.

The samples are chemically cleaned in accordance with the procedure for cleaning tantalum as described in the last quarterly report, (EOS Report 6952-Q-1) with the exception that the hot chromic acid dip should be limited to 4 seconds duration.

2.2.2 Vacuum Outgassing Schedules for Rhenium

The rhenium samples which were prepared as described in the previous paragraphs were mounted in refractory metal firing stands for electron bombardment heating in a vac-ion pumped environment. The firing stands are fitted with high-purity, vacuum-fired rhenium legs which support the samples. Rhenium was selected as the support material to prevent the formation of eutectics or the diffusion of metal support impurities into the process sample during the high-temperature firing operation.

As a starting point for this investigation, an outgassing schedule of 2450°C for 24 hours was selected for the first sample. The second sample was outgassed at 2450°C for 10 hours and the third sample at 2450°C for 3 hours. All temperature measurements were made by viewing the 8:1 hohlraum with a calibrated micro-optical pyrometer. The sample surfaces were subsequently examined on a Zeiss metallograph. Individual grains were marked by a microhardness tester

and photographed without metallographic preparation such as etching or polishing. The samples were returned for 100-hour operation at 1735°C and reexamined on the metallograph.

2.2.3 Surface Stability Examination

The reexamined surfaces, shown in Figs. 2-8b and 2-9b, indicate no surface structure changes with the possible exception of some thermal etching at grain boundaries. There appears to be no significant movement of grain boundaries or evidence of further recrystallization as a result of the 100-hour operation. The fiducial mark which locally stressed the surface in the immediate neighborhood of the mark shows expected signs of stress relief. Note the different appearance in the "before" and "after" photographs. The last rhenium sample, fired at 2450°C for 3 hours, is presently undergoing examination as shown in Fig. 2-10. The larger grain size on the 24-hour and 10-hour samples is evident across the entire surface of each sample and supports the thesis that secondary recrystallization is time, as well as temperature, dependent.

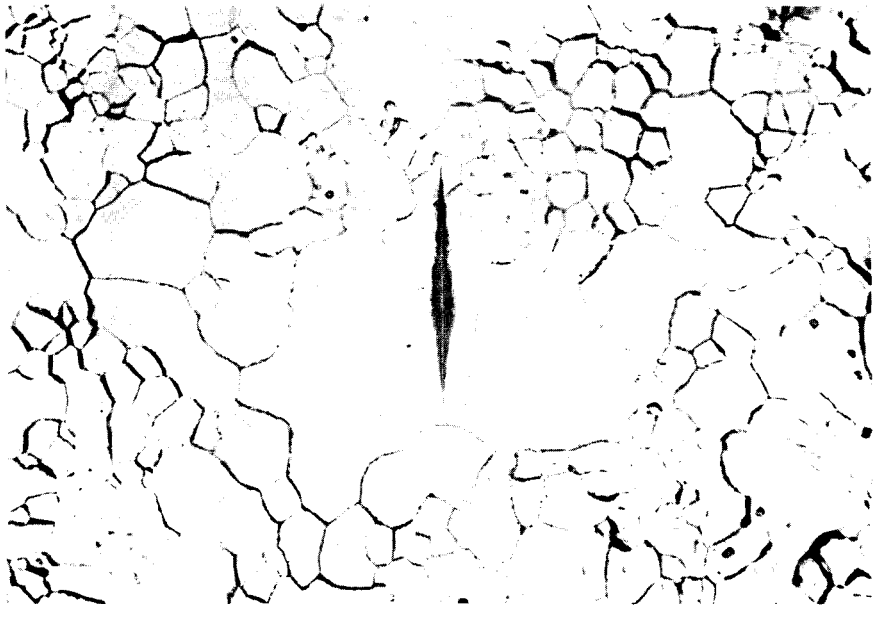

FIG. 2-8a RHENIUM PROCESS SAMPLE VACUUM-FIRED AT 2450°C FOR 24 HOURS IN A VAC-ION PUMPED ATMOSPHERE OF 3 X 10^{-7} TORR. (X200)

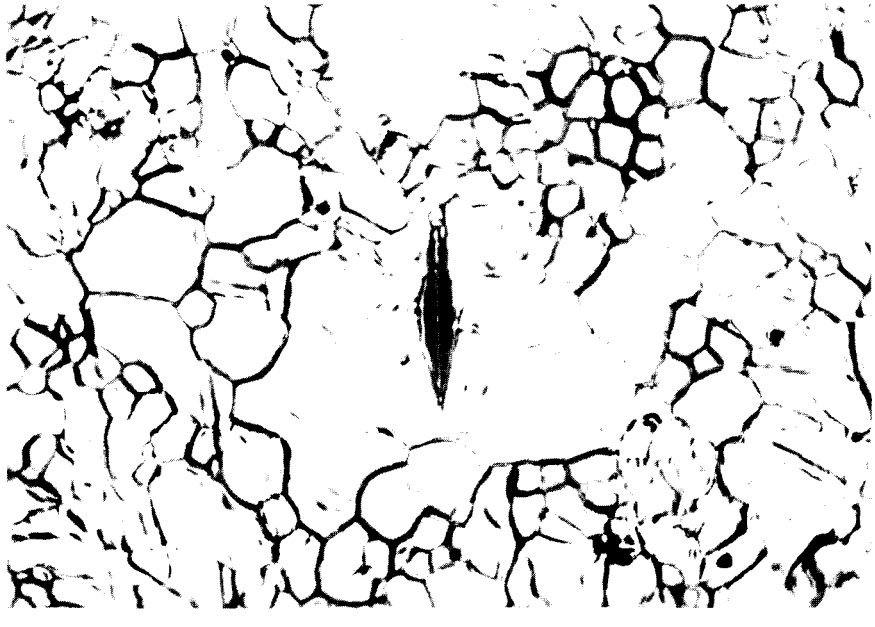

FIG. 2-8b SAME SAMPLE AFTER 100-HOUR OPERATION AT 1735°C IN A VAC-ION PUMPED ATMOSPHERE OF 4 X 10^{-8} TORR. (X200)

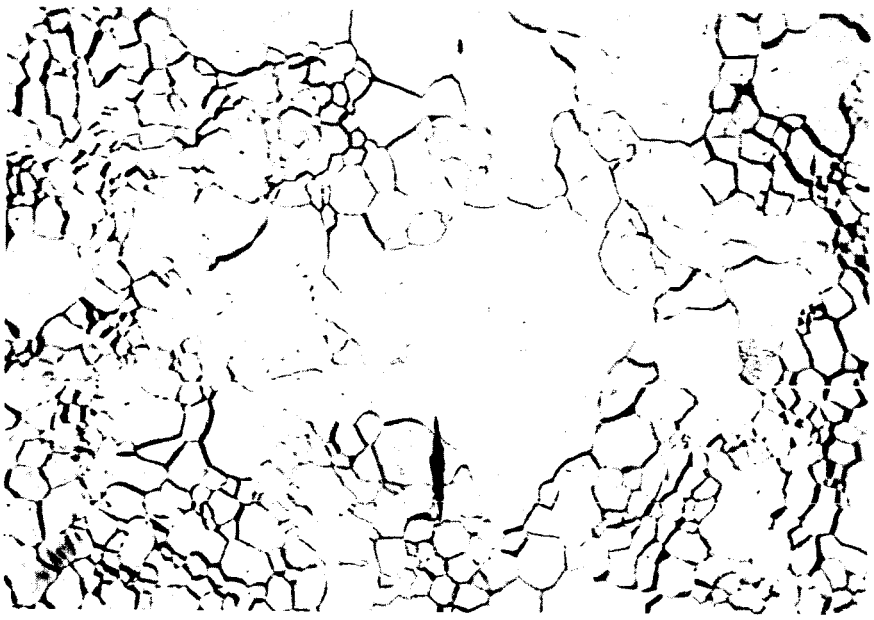

FIG. 2-9a RHENIUM PROCESS SAMPLE VACUUM-FIRED AT 2450°C FOR 10 HOURS IN A VAC-ION PUMPED ATMOSPHERE OF 3 X 10^{-7} TORR. (X200)

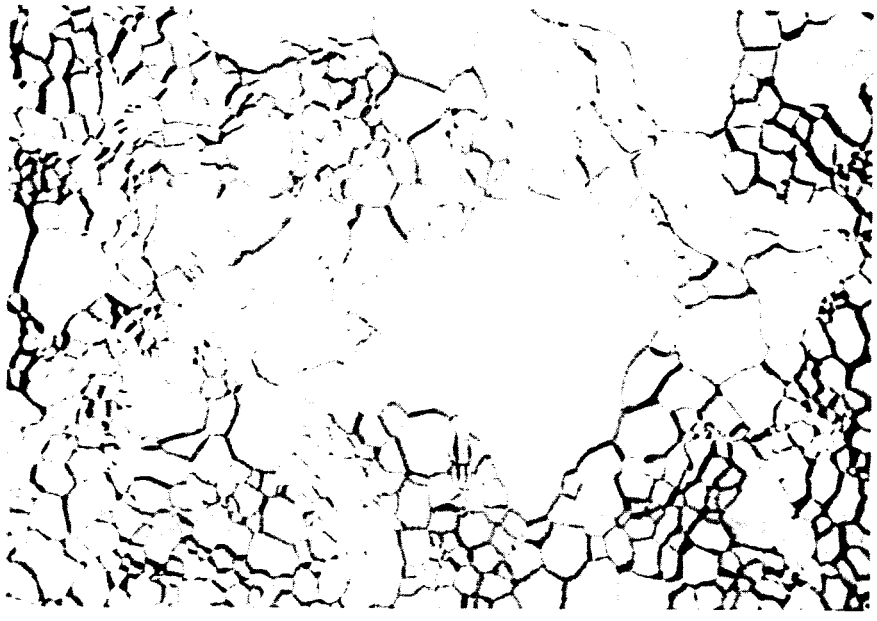

FIG. 2-9b SAME SAMPLE AFTER 100-HOUR OPERATION AT 1735°C IN A VAC-ION PUMPED ATMOSPHERE OF 4 X 10^{-8} TORR. (X200)

FIG. 2-10 RHENIUM PROCESS SAMPLE VACUUM-FIRED AT 2450°C FOR 3 HOURS IN A VAC-ION PUMPED ATMOSPHERE OF 3×10^{-7} TORR. (X250)

3. CONVERTER STUDY AND SECONDARY EXPERIMENTS

3.1 Nonintegral Collector/Radiator Experiments

Electro-Optical Systems converters built during earlier programs contained an integrally forged molybdenum collector radiator to satisfy prototype hardware requirements of mass production and vibration resistance. The integral collector/radiator had a continuous heat transfer path, from collector surface to radiator tip, which was unimpaired by any braze interface. The major disadvantage of the all-molybdenum structure was its weight.

An experimental investigation has been conducted to study the problems of reliably bonding a molybdenum collector to a copper radiating fin. Figure 3-1 is an illustration of the brazed assembly which is nominally of converter size to permit heat transfer rates of 200-225 watts through the braze joint. The molybdenum portion of the assembly is an integrally forged part in which the mounting holes and braze joint are machined. The braze joint is a machined slot designed to captivate the copper radiating fin so that the thermal expansion mismatch keeps the two parts in compression. Shim-stock Nioro (82 percent gold - 18 percent nickel) braze material 0.002-inch thick was inserted in the slot on either side of the copper. A 0.030-inch Nioro wire was placed at the copper-molybdenum intersection on either side of the copper fin. The assembly was vacuum brazed at 925^{o}C, the melting point of Nioro. It was then visually inspected for cracks and was found to contain no voids, cracks, or surface imperfections.

After fabrication, the copper radiator and molybdenum collector root sections were Rokided and instrumented with thermocouples to determine: (1) the bond integrity between the copper-molybdenum as a function of continuous thermal cycling, and (2) the

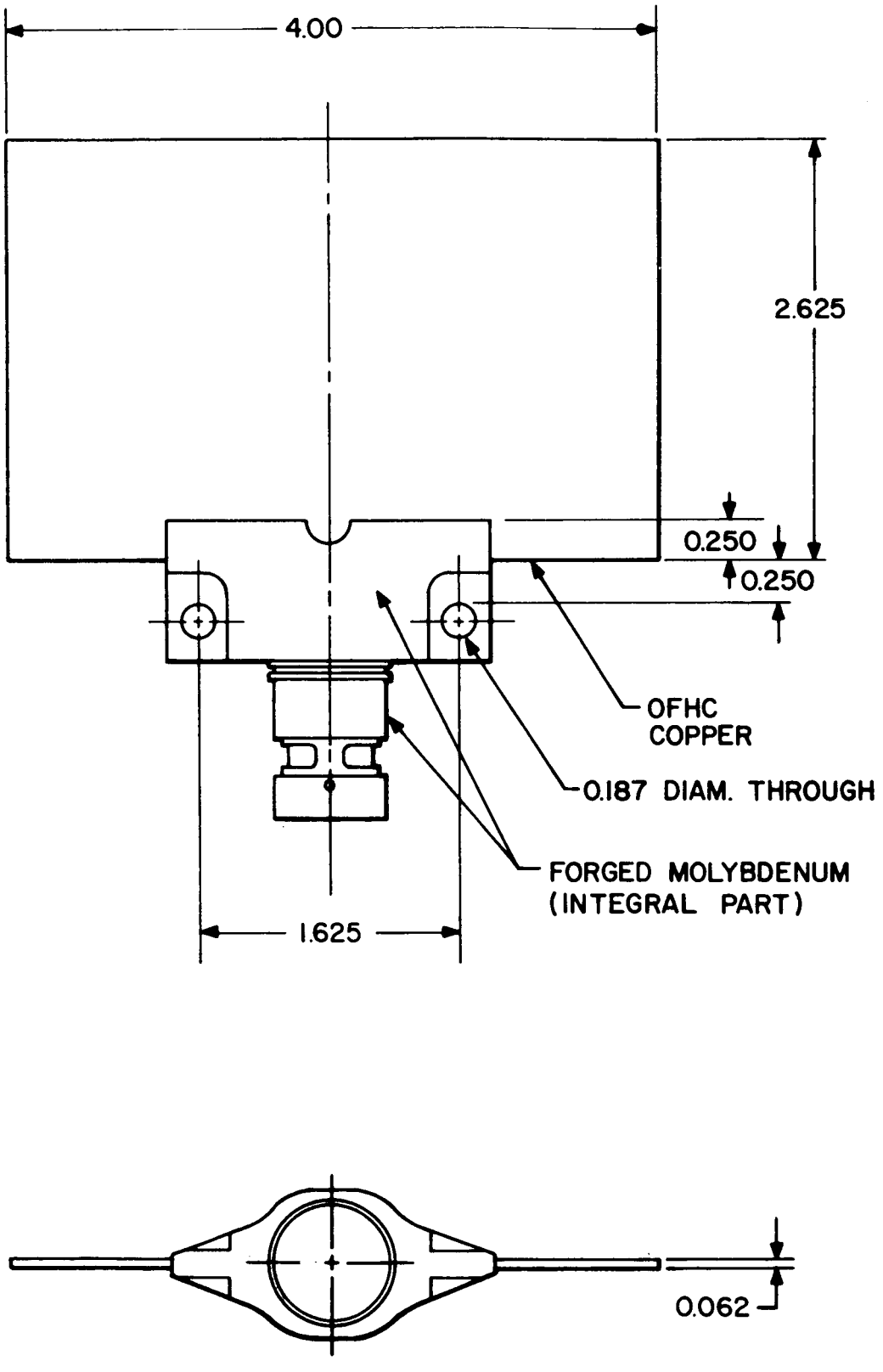

FIG. 3-1 NONINTEGRAL COLLECTOR-RADIATOR ASSEMBLY

thermal dissipation per unit weight of the assembly. The completed assembly was mounted on ceramic sleeves to insure a minimal thermal loss from the structure by conduction. The bond between the copper and molybdenum was subjected to 329 thermal cycles from 600° to 200°C. The thermal cycle was an instantaneous on-off thermal load of 210 watts, with the temperature rise and fall rate limited only by the specific heat and mass of the structure. A temperature drop of 5°C across the braze joint at 210 watts thermal load remained constant throughout the thermal cycles. The temperature drop was measured with six thermocouples located along the braze joint. This performance indicates that a high-quality thermal bond as well as a reliable one has been achieved.

At a collector root temperature of 600°C, the assembly was computed to dissipate about 210 watts. The computation uses an EOS-measured value of 0.78 for the emissivity of Rokide and an "average" radiator spade temperature of 500°C, which is pessimistically low. The weight of the entire assembly is 220 grams, as compared to 230 grams for an integral molybdenum collector-radiator. Therefore, for approximately the same weight, the amount of heat rejected was almost double that of the all-molybdenum EOS production converter collector-radiator which dissipated about 120 thermal watts.

The nonintegral assembly will be reexamined for temperature distribution after some of the copper spade is removed. The thermocouple measurements indicate, as expected, that the lowermost corners of the radiator are operating at a temperature (425°C) which is too low for efficient radiation heat rejection. After all experimental measurements are concluded, the brazed molybdenum-copper joint will be metallurgically examined for void structures and brittle phases.

3.2 Converter Fabrication Investigations

3.2.1 Converter Seal-Off

An experimental investigation has been concluded which establishes the necessary procedures for effecting a highly reliable converter seal-off. Copper tubulation seal-offs performed in the past with the aid of hand-operated pinch-off tools have always been vacuum tight but of marginal seal-off area.

The seal-off operation is performed with a pinch-off tool which applies pressure sufficient to cold-weld the converter reservoir tubulation. The cold-weld illustrated in Fig. 3-2 is leak tight and has the external appearance of being a good pinch-off. In microsection, however, the minimum seal thickness is found to be only 0.001 inch. A pinch-off such as this is considered marginal since it cannot suffer any accidental damage in the pinch-off area without loss of the vacuum seal on the converter.

Six pinch-offs were made with two different hand tools (Varian and Kane). The pinch-offs were then cross-sectioned, and metallurgically examined for seal thickness. Of the six pinch-offs, only one sample had a seal thickness greater than 0.005 inch, the rest were 0.001 inch or less. In general, the hand tools required continuous adjustment to insure that the rollers mated properly. The rollers, though case-hardened, require periodic replacement. The actual pinch operation utilizing a hand tool is dependent upon the steadiness and skill of the operator.

Six pinch-offs were made from the same length of sample tubing. The tool used for these pinch-offs was a Kane hydraulic tool having 1/4-inch and 1/8-inch diameter, fully hardened tool-steel rollers. All pinch-off samples were examined for seal thickness and were found to vary between 0.006 inch and 0.009 inch with no preference for roller diameter (Figs. 3-4 and 3-5). The hydraulic tool requires only initial adjustment and occasional readjustment; the rollers appear

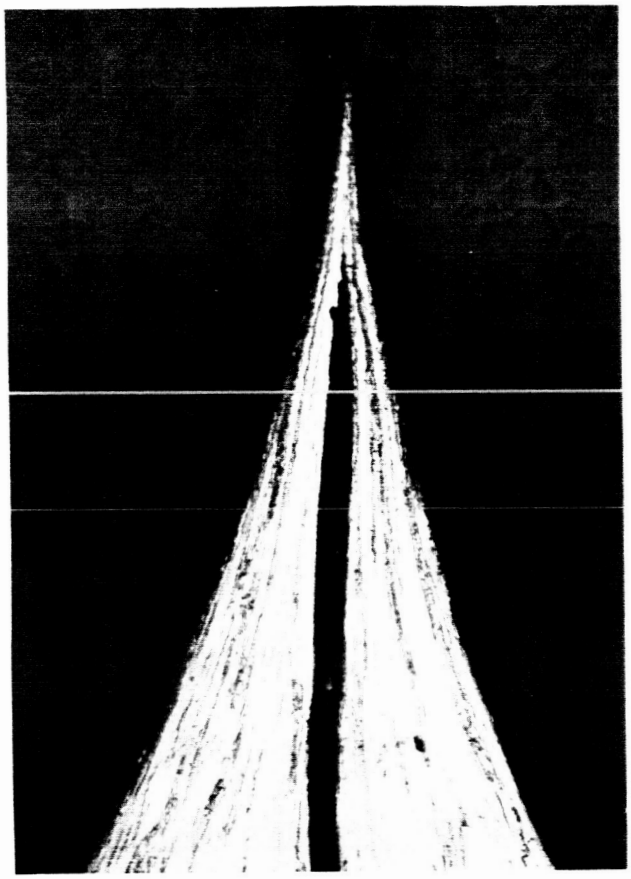

FIG. 3-2

ANNEALED OFHC COPPER TUBING 1/4" O.D., 0.030" WALL. KANE HAND PINCH-OFF TOOL. (X75)

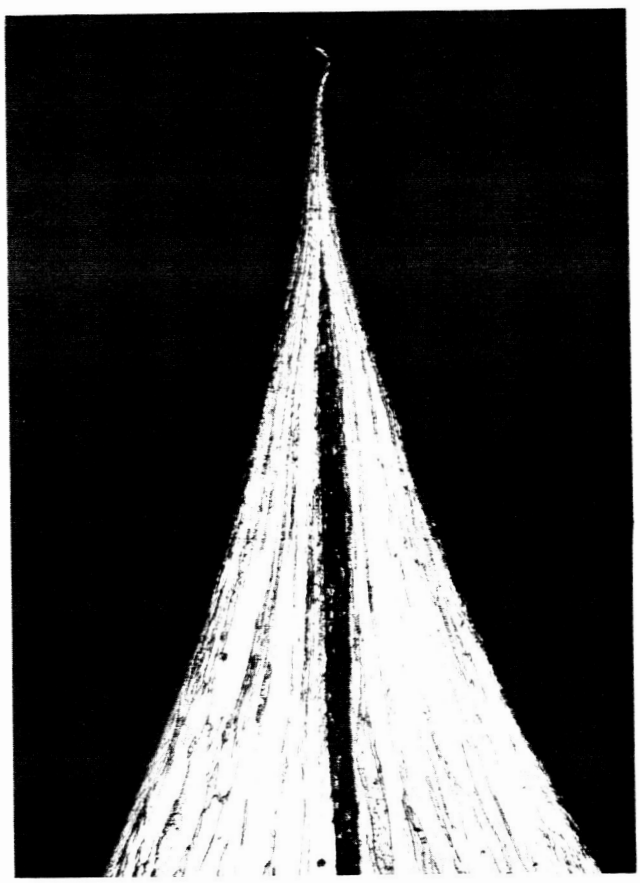

FIG. 3-3

ANNEALED OFHC COPPER TUBING 1/4" O.D., 0.030" WALL. VARIAN HAND PINCH-OFF TOOL. (X75)

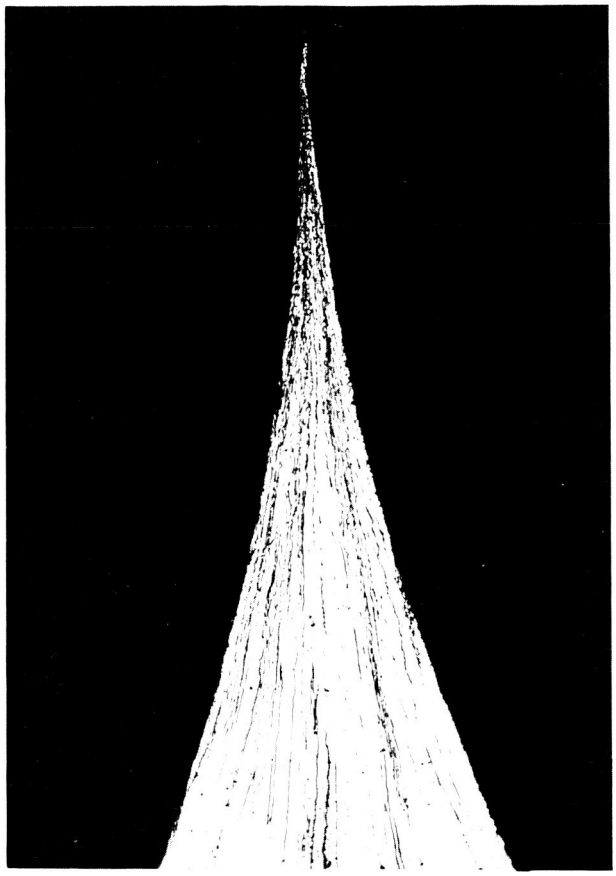

FIG. 3-4

ANNEALED OFHC COPPER TUBING 1/4" O.D., 0.030" WALL. KANE HYDRAULIC PINCH-OFF TOOL WITH 1/4"-RADIUS ROLLER. (X100)

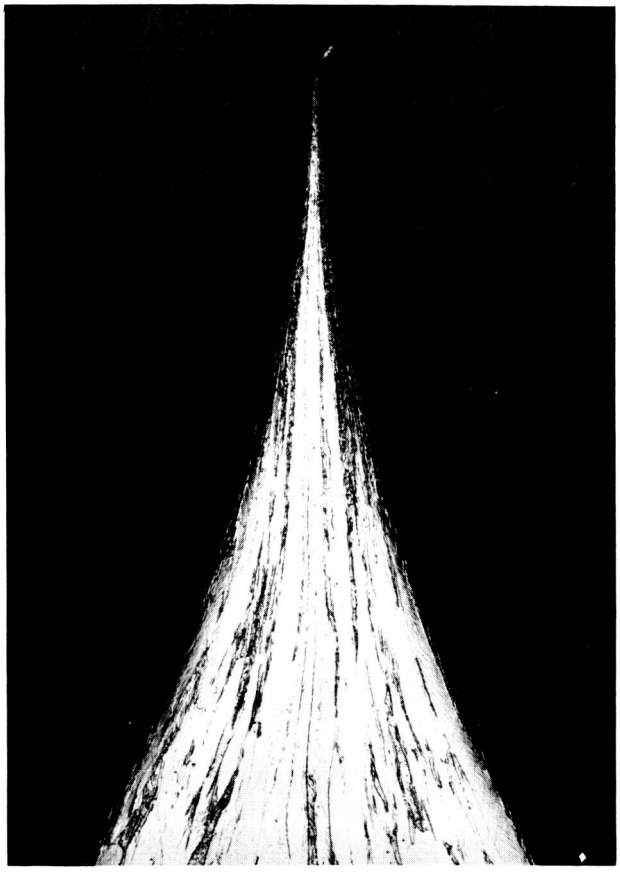

FIG. 3-5

ANNEALED OFHC COPPER TUBING 1/4" O.D., 0.030" WALL. KANE HYDRAULIC PINCH-OFF TOOL WITH 1/8"-RADIUS ROLLER. (X75)

to be capable of lasting almost indefinitely and the pinch-off operation proceeds with a smooth stroke, independent of operator skill or experience.

A few general observations on pinch-off procedures are outlined below which, if followed, should lead to consistent, highly reliable OFHC copper tubing pinch-offs.

1. The copper (OFHC) must be first chemically cleaned to remove all contamination induced by mill handling.
2. The copper must be fully annealed (after chemical cleaning) in a high-vacuum environment at temperatures in the 700°C range for 1/2 hour.
3. The pinch area should be preflattened with a flattening tool and re-annealed.
4. The pinch-off rollers or jaws should be made of fully treated tool steel and they should be periodically checked for evidence of warpage or misalignment.
5. The pinch-off tool should be hydraulically actuated to provide maximum sealing area and consistent pinching action.

3.2.2 Ceramic-Metal Seals

A ceramic-metal seal study is being conducted to examine seal reliability upon repeated thermal shock. The study is confined to the niobium-alumina system active alloy brazed with nickel zirconium. In addition, some assemblies will be operated at elevated temperatures to obtain life-time data.

Three seal assemblies have been fabricated and leak tested with a helium mass spectrometer leak detector of calibrated sensitivity in the 10^{-10} Std.-cc/sec range. Each assembly consists of two niobium flanges with a right-angle spun surface that is flat to within 0.001 inch. An alumina ring of high-purity (Wesgo AL-995) and precision flatness (less than 0.0005 inch) was sealed between the niobium flanges with a eutectic mixture of nickel and zirconium. Brazing was accomplished

in accordance with Specification GMP-34200/020-GEN. The assemblies were identical in dimensions, except that the flange for each assembly was 0.020 inch, 0.030 inch, and 0.040 inch thick, respectively, as compared to previous EOS production and experimental converter flanges with 0.010-inch thicknesses. It has been found that thicker flanges preserve and improve structural rigidity of the converter in the absence of the retaining ring.

The testing program and its results are summarized below:

1. The 0.020-inch-thick niobium flange-alumina seal assembly was thermally cycled 250 times from 220°C to 610°C at a rate of 100°C/min and tested leak tight.
2. The 0.030-inch-thick niobium flange-alumina seal assembly was thermally cycled 252 times from 220°C to 610°C at a rate of 100°C/min and tested leak tight. This assembly was subsequently operated for 500 continuous hours at 700°C and tested leak tight. These tests are continuing.
3. The 0.040-inch-thick niobium flange-alumina seal assembly was thermally cycled 189 times between 200°C and 600°C at 100°C/min and tested leak tight. The assembly was subsequently cycled to a total of 289 times under the same cycling conditions. The ceramic cracked during the last 100 cycles.

The 0.020-inch and 0.030-inch-thick niobium flange-alumina seals have performed well under conditions of moderate to severe thermal shock for a ceramic-metal seal assembly (alumina itself is limited to heating and cooling rates of 200°C/min). In addition, the active alloy seal appears to be capable of long-life operation at elevated temperatures.

The parts for a cesium-filled seal assembly have been fabricated and are being assembled to assess the seal resistance to thermal shock and elevated temperature in a high-pressure cesium environment (i.e., at pressures of 10 to 20 mm Hg). Voltage breakdown

measurements as a function of pressure will be recorded during the tests as a method of determining the seal integrity. It is anticipated that any seal leak incurred during device operation will shift the minimum position of breakdown due to the introduction of impurities into the cesium vapor.

3.2.3 Electron-Beam Welding of Rhenium-Rhenium Samples

An experimental investigation to establish proper schedules for rhenium-to-rhenium electron-beam welding has been completed. The most immediate application of this investigation was the successful welding of the test vehicle rhenium envelope to the rhenium emitter without parts loss or reweld attempts.

Two rhenium sheet strips, each 0.020-inch thick, were ground flat, chemically cleaned, and clamped together to serve as feasibility samples for different electron-beam parameters. Five separate weld passes of minimum spot diameter (0.012 inch) were made on the EOS Hamilton-Zeiss electron-beam welder in a 4×10^{-5} torr vacuum environment. Figure 3-6 illustrates that a beam power of 150 kV x 3.4 mA at a part speed of 100 in/min is not sufficient to achieve penetration into the bottom part. However, a reduced part speed of 90 in/min for the same beam power produced penetration, as shown in Fig. 3-7. A higher beam power and lower parts speed of 150 kV x 4.7 mA at 80 in/min yields good penetration into the bottom sheet as shown in Fig. 3-8. It is interesting to note that while the weld (shown in Fig. 3-7) would be leak tight, the degree of bonding is much greater for the latter schedule. Figure 3-9 illustrates the effect of a weld schedule sufficient to cause blow-through in the bottom sheet. The recommended schedule for electron-beam welding a 0.020-inch-thick rhenium envelope to a rhenium emitter is 150 kV x 4.9 mA at a part speed of 80 in/min. If the weld is circumferential, the part speed, which is linear in this investigation, would be corrected to revolutions/min. A minimum electron-beam

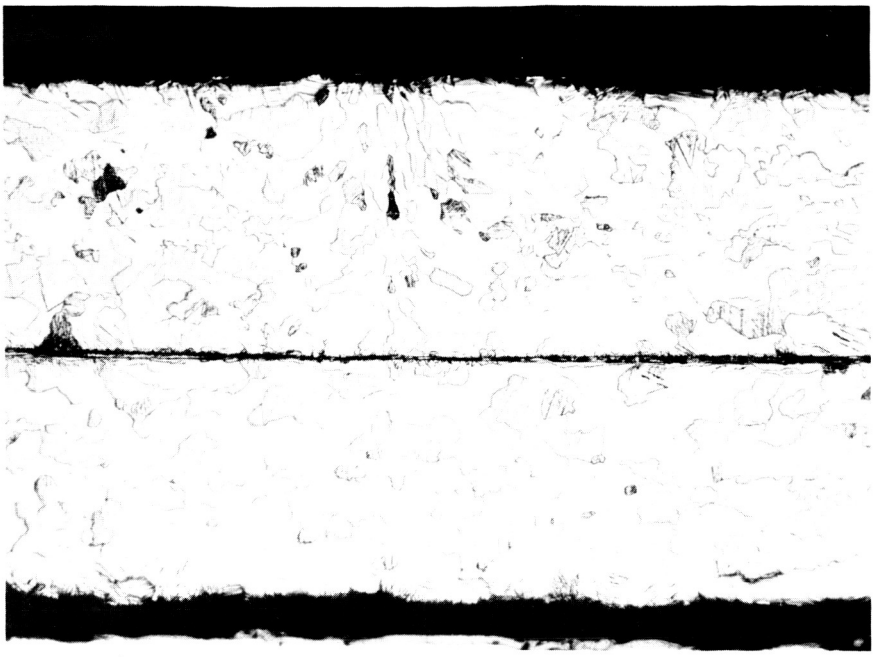

FIG. 3-6 RHENIUM SHEET TO RHENIUM SHEET ELECTRON-BEAM WELD. BEAM VOLTAGE OF 150 KV X CURRENT OF 3.4 MA. PART SPEED OF 100 IN/MIN. (X75)

FIG. 3-7 RHENIUM SHEET TO RHENIUM SHEET ELECTRON-BEAM WELD. BEAM VOLTAGE OF 150 KV X CURRENT OF 3.4 MA. PART SPEED OF 90 IN/MIN. (X75)

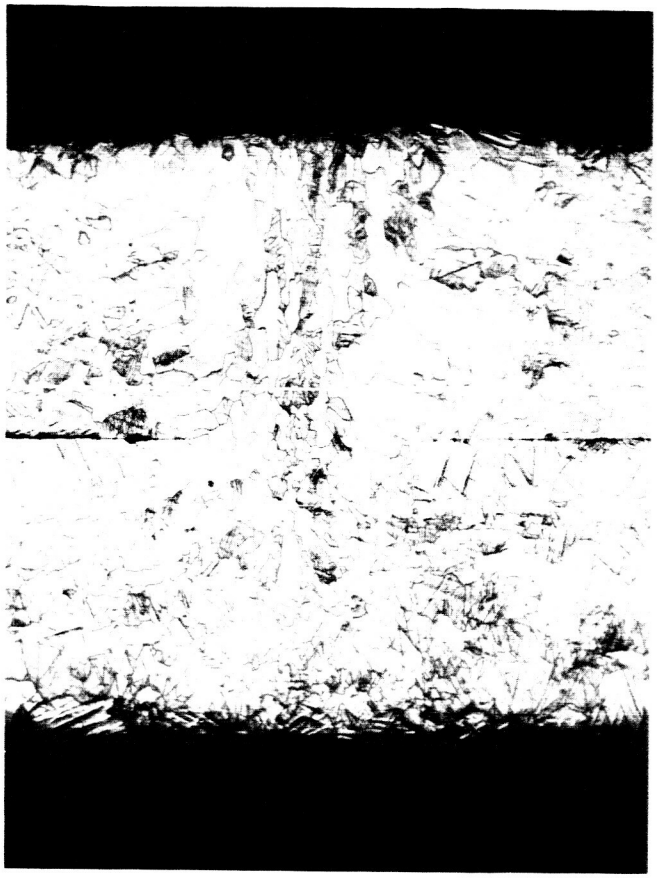

FIG. 3-8

RHENIUM SHEET TO RHENIUM SHEET ELECTRON-BEAM WELD. BEAM VOLTAGE OF 150 KV X CURRENT OF 4.7 MA. PART SPEED OF 80 IN/MIN.

FIG. 3-9

RHENIUM SHEET TO RHENIUM SHEET ELECTRON-BEAM WELD. BEAM VOLTAGE OF 150 KV X CURRENT OF 6 MA. PART SPEED OF 80 IN/MIN.

diameter of approximately 0.012 inch is recommended for this type of welding since such a beam is more easily controlled and requires less total beam power to achieve the same penetration. The standard practice of requiring clean parts and good fit is essential to electron-beam welding.

3.2.4 Interelectrode Spacing

An investigation is being conducted to obtain direct measurements of the interelectrode spacing of a converter structure simulating the thermal conditions found during high-performance electrical operation. A high-magnification, high-resolution optical system complete with micrometer drum drive, will be employed to measure the distance between the electrodes of a converter structure. To this end, a thermal mockup of converter SN-101 has been fabricated with viewing slits to allow optical measurement of interelectrode spacing as a function of emitter and collector temperature.

Since the spacing of a converter depends upon the thermal expansion differences between the emitter support structure and the collector, the temperature distribution of these elements must, therefore, be identical to those experienced in actual converter operation. Emitter temperatures will be measured with a micro-optical pyrometer. Collector temperatures will be measured with two immersion thermocouples at a point 0.050 inch from the collector surface. Element temperatures such as the collector root and emitter lead strap (or seals) will be measured by thermocouples.

The mockup parts for this experiment have been fabricated and are presently being instrumented for test. The optics for measuring the spacing have been bench tested by viewing a ruled grid. The measurements indicate that accuracies of ±0.0001 inch are readily obtained.

The final measurements from this investigation will be used to check the accuracy of calculating the interelectrode spacing

from measured temperature distributions and thermal expansion considerations. For example, the interelectrode spacing calculated for the thermal mockup of converter SN-101 is 0.0015 to 0.002 inch assuming that:

1. The electrodes are in contact at room temperature and that there are no residual stresses in the supporting structure.
2. The temperature gradient on the envelope is equivalent to previous gradient measurements.

4. CONVERTER DESIGN (SN-101)

The thermionic converter design goals for this program are listed below:

1. A power output density of 20W/cm^2 at 0.8 volt from a 2.0 cm^2 emitter area. The emitter temperature for this output is 1735°C true, as measured in an 8:1 depth-to-diameter black-body hole with corrections for bell jar transmission loss.
2. An efficiency of 14 percent, measured at the conditions of output power density just described, using a flat, counter-wound, 0.020-inch-diameter tungsten filament.
3. Minimum converter weight consistent with a four-converter generator weighing a total of 4 pounds.
4. Improved heat transfer from the converter collector surface to the radiator and sufficient radiator area to reject the generated heat loads during dc operation of the converter. No conduction cooling should be resorted to during electrical performance test.

The design and fabrication of the converters are proceeding in an iterative fashion wherein each converter is designed utilizing operational information from previous converters, the variable-parameter vehicle data and the secondary experiments.

The first set of converter electrode materials is rhenium-rhenium, both from the same vendor source and mill number to establish material control. The collector is a thin shim of rhenium approximately 0.040-inch thick, vanadium brazed to the molybdenum barrel. The rhenium emitter is supported by rhenium tubing to avoid contamination of the emitter surface (with materials such as tantalum) which occur by surface diffusion at high temperature.

The following paragraphs discuss the design particulars of converter SN-101.

4.1 Converter Efficiency

The efficiency of converter SN-101 is calculated by way of standard consideration in the following manner:

$$\eta = P_{out}/P_{elec\ cool} + P_{rad} + P_{cs\ cond} + P_{env\ cond} \quad (1)$$

where P_{out} is set at 20 watts/cm^2 from 2 cm^2, $P_{elec\ cool}$ is the thermal power carried away from the emitter by electrons "evaporating" from the emitter surface, P_{rad} is the net heat lost from the emitter surface by radiation, $P_{cs\ cond}$ is the net thermal "gas" conduction loss from the emitter surface, and $P_{env\ cond}$ is the conduction heat transferred from the emitter to its envelope support structure.

Each of the loss terms is now examined at the power output design point.

$$P_{elec\ cool} = I\ (\phi_{eff} + 2kT/e) \quad (2)$$

where ϕ_{eff} is the effective emitter work function obtained from the Richardson-Dushman equation by setting A, the pre-exponential multiplier, equal to 120 amperes/cm^2 — $^oK^2$; T, the emitter temperature, at 2000^{o}K; and J_s, the saturated electron emission, at 25 amps/cm^2.

$$J_s = A\ T^2 e^{-e\phi/kT} \quad (3)$$

$$\frac{25\ \text{amps}}{\text{cm}^2} = \frac{120\ \text{amps}}{\text{cm}^2\ -^oK^2} \times 4 \times 10^6 -^oK^2\ e^{-\frac{1.6 \times 10^{-12}\ \phi_{eff}}{1.38 \times 10^{-16} \times 2 \times 10^3}}$$

solving for ϕ_{eff},

$$\phi_{eff} = 2.9 \text{ volts}$$

The term 2kT/e is an additive energy term, divided by the electron charge for conversion to units of potential energy, which accounts for the energy distribution of emitted electrons. For an emitter temperature, T, of 2000^{o}K this additive term is equal to 0.32 volt.

The total electron cooling loss for 2.0 cm^2 with a 50-ampere current is:

$$P_{elec\ cool} = 50\ (2.9 + 0.32) = 160 \text{ watts}$$

$P_{rad}/cm^2 = e_{eff}\sigma(T_{em}^4 - T_{coll}^4)$ where e_{eff} is the effective emissivity of the electrode system which has been determined previously (Ref. 1) to be 0.16.

$$P_{rad} = 0.16 \times 5.7 \times 10^{-12} \times \left[(2 \times 10^3)^4 - (1.1 \times 10^3)^4\right]$$

$$P_{rad} = 13 \text{ watts/cm}^2$$

For 2.0 cm^2, the heat loss from the emitter surface is 26 watts.

The power loss via cesium conduction loss has been experimentally reported to be 10 watts in the cesium pressure range of interest (i.e., from 2 to 10 mm Hg).

The final loss term to be considered is the envelope conduction, $P_{env\ cond}$. The design of the envelope, which acts as the emitter support structure as well as the emitter lead strap, requires a compromise between the electrical losses and thermal losses. The usual lead analysis, which follows, derives an L/A ratio for the envelope which is obtained by examining the ratio of electrical to thermal losses. Let α be defined as the ratio of electrical to thermal loss:

$$\alpha = \frac{I^2 \rho\ L/A}{K\Delta T\ (\frac{A}{L}) - 1/2\ I^2 \rho\ (\frac{L}{A})} \qquad (4)$$

The thermal loss term in the denominator is the sum of the simple heat conduction minus half the joule heating losses since the joule heating losses will modify the envelope temperature distribution in a manner which will reduce the straight conduction loss. For an α value of 0.1, the L/A ratio for a rhenium envelope with $\rho = 80 \times 10^{-6}$ ohm-cm, K = 0.48 watt/cm - ^oC, I = 50 amperes, and $\Delta T = 1000^oC$ is:

$$L/A = \frac{1}{50}\sqrt{\frac{0.48 \times 0.1 \times 1000}{80 \times 10^{-6}\,[1 + 1/2\,(0.1)]}}$$

$$L/A = 15\ cm^{-1}$$

From a fabrication standpoint, an envelope wall thickness of less than 0.003 inch is difficult to produce with a high yield. Therefore, a minimum wall dimension of 0.003 inch has been selected and the resultant length, L, is approximately 0.22 inch for an envelope diameter of 0.631 inch. The electrical loss $I^2 \rho\ L/A$, by substitution, is $(50)^2 \times 80 \times 10^{-6}$ ohm-cm $\times\ 15\ cm^{-1} = 3$ watts, while the thermal loss, or $P_{env\ cond}$, is 30 watts.

Returning to the efficiency expression, η may be written as:

$$\eta = \frac{40 \text{ watts}}{160 \text{ watts} + 26 \text{ watts} + 10 \text{ watts} + 30 \text{ watts}}$$

$$\eta = 18 \text{ percent}$$

which compares to the program goal of 14 percent with bombardment gun losses.

An EOS converter, fabricated and tested on Contract JPL 950699, which had a power output density of 20 watts/cm^2 at a terminal voltage of 0.7 Vdc, yielded an efficiency of 11 percent when measured according to the methods defined in the present program design goals. However, the converter current level on that particular test was higher since the power output was obtained at an output voltage of 0.7 Vdc instead of 0.8 Vdc. If a lower current level could have been established for the same output power, the projected test efficiency would have been 13.8 or 14 percent measured.

4.2 Collector-Radiator Structure

The collector-radiator structure for converter SN-101 has been selected as a brazed molybdenum-copper assembly to satisfy the design objectives of minimum weight and increased heat rejection without conduction cooling. Previous EOS converters employed an integral molybdenum

collector-radiator which was compact and possessed high strength at temperature. In addition, the structure was die forged in production lots to reduce converter manufacturing costs. The only disadvantage of the all-molybdenum structure was that a converter operating at the $20 W/cm^2$ (thermal) power level would weigh over 500 grams.

As a starting point in the collector-radiator design, it is necessary to calculate the collector heat load that must be rejected at the dc design operating point of 50 amperes. The following paragraphs contain these calculations and re-examine the molybdenum-copper spade in terms of heat rejection per unit weight.

4.2.1 Collector Heat Load

The collector heat load, Q, may be written as the sum of three terms:

$$Q = Q_{el\ ht} + Q_{rad} + Q_{cs\ cond} \tag{5}$$

where $Q_{el\ ht}$ is the heat generated by the drift current electrons in transit from the plasma, a region of higher potential energy, to the collector Fermi level, a region of lower potential energy. In concept, it is exactly opposite to the electron cooling term associated with the emitter, wherein electrons being lifted from the emitter Fermi level to the virtual emitter, remove heat from the emitter in the process. The terms Q_{rad} and $Q_{cs\ cond}$ are equivalent to those discussed in the analysis of heat lost from the emitter. $Q_{el\ ht}$ may be written as:

$$Q_{el\ ht} = kI, \tag{6}$$

where I is the drift or output current and k is defined as the summation of the kinetic energy of the plasma electrons and the potential energy fall represented by the effective work function of the collector.

$$k = \frac{4kT_{pl}}{\pi e} + (Q_{coll} \pm V_s)^0 \tag{7}$$

A discussion of the origin and nature of the plasma potential energy term is presented in the Appendix. For an electron plasma temperature of $6000^{\circ}K$

$$\frac{4kT_{pl}}{\pi e} = \frac{4 \times 1.38 \times 10^{-16} \times 6000}{\pi \times 1.6 \times 10^{-12}} = 0.66v$$

The measured minimum work function of cesium on rhenium has been determined to be 1.47 volts. Setting the collector sheath at zero for optimized operation, k is determined as;

$$k = 0.66 \text{ v} + 1.47 \text{ v}$$

$$k = 2.13 \text{ v}$$

and

$$Q_{\text{el ht}} = 2.13 \text{ (50 amps)}$$

$$Q_{\text{el ht}} = 107 \text{ watts for 50 amperes current load.}$$

To operate at 70 amperes without conduction cooling, the radiator would be required to reject a total heat load, Q, of

$$Q = (2.13)\ 70 \text{ watts} + 26 \text{ watts} + 10 \text{ watts}$$

the latter two terms being Q_{rad} and $Q_{cs\ cond}$

$$Q = 190 \text{ watts}$$

4.2.2 Radiator Heat Rejection

The molybdenum collector-copper radiator discussed previously in Section 3 provides a full-scale test for rejection of the computed collector heat load of 200 watts. The results of the testing program are repeated as follows:

1. At a collector root temperature of 600°C, 200 - 225 thermal watts were dissipated by radiation.
2. The structure was thermal-cycled (on-off) 350 times under heat rejection loads of 200 - 225 watts. A ΔT of 4°C - 8°C across the molybdenum-copper interface was measured before and after thermal cycling.
3. No deterioration of the Rokide coating was observed.

The structure just described weighed 220 grams compared to the all-molybdenum collector-radiator weight of 250 grams. The

all-molybdenum system dissipated 125 watts thermal at the design point of 12.5 W/cm^2 electrical. The molybdenum-copper system is, therefore, capable of rejecting twice the heat load of the molybdenum system and at the same weight. A total weight of 240 grams is estimated for converter SN-101, yielding a specific power of 13 lbs/KW(e) for the converters.

4.3 Interelectrode Spacing Considerations

There are several sources of data relating to the optimum interelectrode spacing for arc-mode thermionic converters. As early as 1961, measurements were taken (Ref. 2) which indicated that a pressure-distance (pd) product of approximately 20 mil-torr produced a plasma with minimum internal voltage loss in an operating cesium vapor thermionic converter. Subsequent measurements (Refs. 3 and 4) have corroborated the gas discharge nature of the cesium vapor thermionic converter and the optimum pressure-distance product at $17 \leq pd \leq 23$ mil-torr.

In apparent contradiction to these pd measurements is the accumulated experience of many of the converter suppliers, which essentially is that: The closer the spacing, the higher the power output. This statement is true, but requires qualification if the level of the voltage at maximum power is a consideration. The majority of converters built and tested have had tantalum-molybdenum electrode systems. SET converters fabricated as early as 1962-1963 with interelectrode spacings of 0.003 inch delivered less power output than converters spaced at 0.002 inch and 0.001 inch. With 0.001 inch established as the lower spacing limit, the philosophy germinated that "the closer the spacing, the higher the power output." However, spacings less than 0.001 inch have been too difficult to reproducibly obtain in converters and the region from 0.001 inch to 0.0005 inch (or less) is ill-defined for the tantalum-molybdenum system. The majority of converters built with a 0.001-inch spacing have optimized performance at, or near, cesium reservoir temperatures from 390°C to 400°C, which corresponds to a pressure of 18 torr. The pd product is, therefore, 18 mil-torr and is in agreement with earlier measurements.

Table I is a summary of the known data concerning the cesiated emission from rhenium at emitter temperatures of 2000°K. The average cesium pressure required to obtain a design point current density of 25 amperes/cm^2 at maximum voltage output is 5 torr. Since a pd relationship or similarity relationship of $\sim$ 20 mil-torr is valid for all electrode materials, sizes, and essentially planar geometries utilizing cesium vapor arc discharges, the optimum interelectrode spacing for the rhenium system operating at 25 A/cm^2 and 0.8-volt output should be:

$$p_1 d_1 = p_2 d_2; \quad d_2 = \frac{p_1 d_1}{p_2}; \quad d_2 \cong 4 \text{ mils} \cong \frac{20 \text{ mil-torr}}{5 \text{ torr}}$$

As an addendum to the interelectrode spacing discussion, there is the possibility of experimental vehicles being operated at such close spacing (less than 0.3 mil) that a plasma is not fully developed and the I-V characteristic is essentially that of a vacuum close-spaced converter. EOS has built and operated such converters with power output densities of 30-33 watts/cm^2 at 1.0 volt terminal voltage for an emitter temperature of 2020°K. However, these devices cannot be reproducibly fabricated at the present time and fall outside the realm of real thermionic hardware.

4.4 Prefabricated Seals

As a method of improving converter fabrication, the design of SN-101 will include prefabrication of the ceramic-metal seals, their pretest, and assembly into the final converter configuration utilizing electron-beam welding. Converters built on previous programs were dependent upon the ceramic-metal sealing operation as the final assembly step. Two disadvantages result: first, a seal failure generally renders one subassembly, and perhaps two, useless with minimal chance of recovery. Second, the vapor pressure of brazing materials is often high enough at the melting point (in the case of copper, 1/2 micron) that the converter interior, including the electrodes, can be coated with several monolayers of braze materials. This coating is unimportant in considering the emitter, but is very important in consideration of the collector which does not operate at high enough temperatures to evaporate many of the contaminants.

TABLE I

CESIATED EMISSION FROM RHENIUM

Investigator	J_{sat} (amps/cm^2)	T_{cs} (^oC)	P_{cs} (mm Hg)	T_{emit} (^oK)
Wilson (G.E.)	35	340	5	2000
Rasor (T.E.C.)	33	342	5	2000
EOS	32	327	3	2000

On the other hand, ceramic-metal seals which are prefabricated in lots of a dozen, may be leak-checked and thermal-cycled, if desired, and stored until final fabrication. The final fabrication would consist of electron-beam welding these prefabricated seals onto the converter structure. The seal testing program, as described in Section 3, has illustrated the rugged and reliable nature of the nickel-zirconium braze of high-purity alumina to niobium. This braze alloy has been selected for prefabricating converter SN-101 ceramic-metal seals.

4.5 Assembly Procedure

Figure 4-1 is a cross-sectional view of the converter. It illustrates the principal features and dimensions of SN-101. The radiator structure is not shown in its entirety but it is identical to the radiator in Fig. 3-1.

The collector subassembly is comprised of the collector barrel, a niobium welding ring, a shim of rhenium plate stock on the collecting surface and a tantalum reservoir with heater wire; all of which are vanadium brazed to the molybdenum barrel. Vanadium has been chosen since it bonds to rhenium without the formation of a brittle intermetallic or low-melting-point eutectic alloy. The other components are vanadium brazed to eliminate step brazing. In addition, vanadium will replace titanium as a metal-to-metal joining material in SN-101 since the α-β phase transition of titanium has been suspected of causing a loss in structural integrity over repeated thermal cycling. The niobium welding ring is selected since its sole function is to provide base material identical to that used to beam weld one flange of the prefabricated seal.

To date, cylindrical parts of niobium and molybdenum have not been welded leak tight, although sample welds of flat stock have shown good penetration.

The envelope subassembly is comprised of a rhenium envelope, a niobium transition section and a tantalum lead strap; all vanadium brazed in one operation. The niobium transition section contains a lip section 0.060-inch thick, to which the upper flange of the prefabricated seal is electron-beam welded.

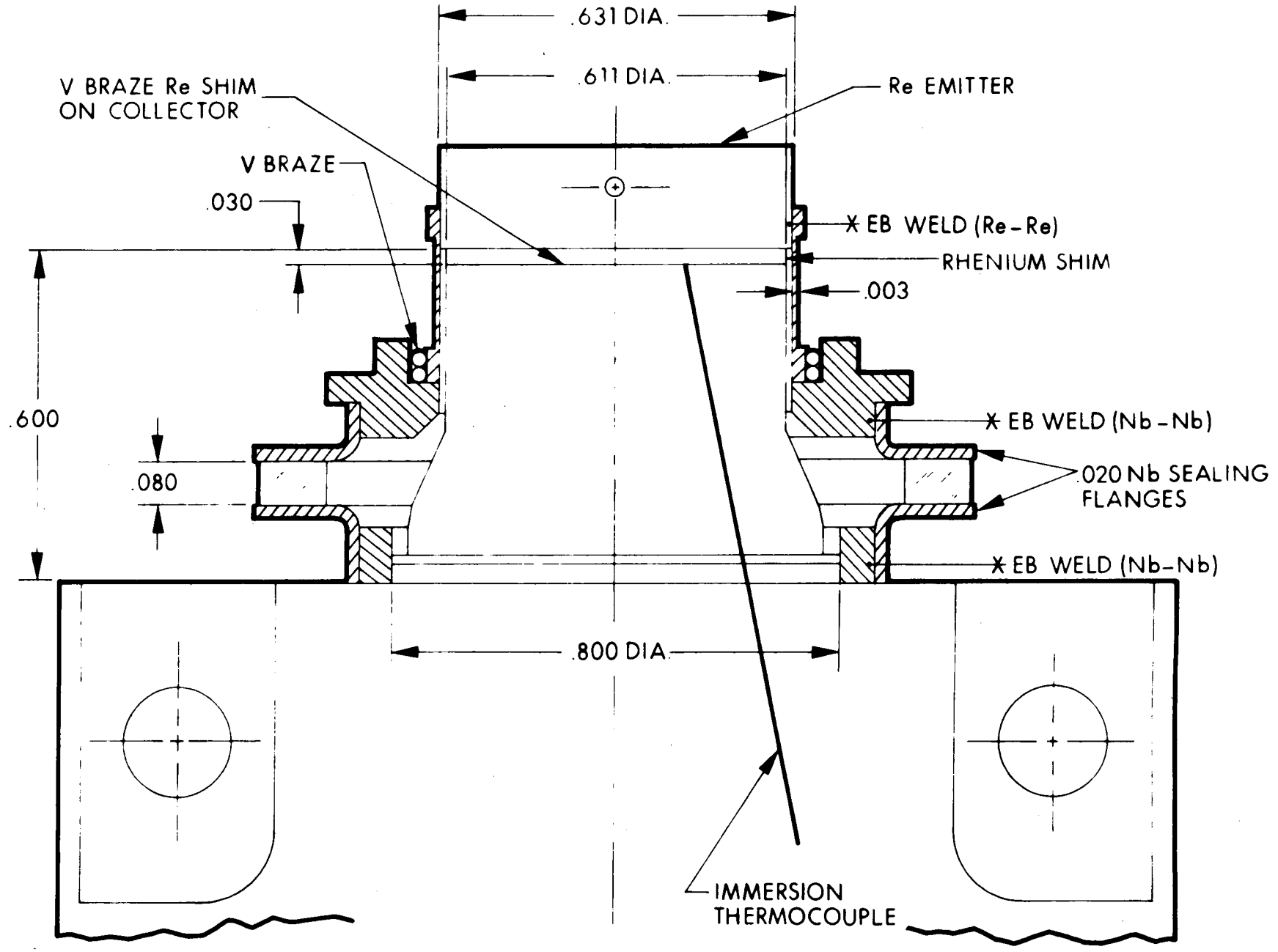

FIG. 4-1 CONVERTER SN-101 DESIGN

The rhenium emitter is positioned in place and electron-beam welded to the rhenium envelope as the final assembly step. At this point, a predetermined spacing may be built into the converter by grinding a ledge on the emitter button. This ledge, located at the right height on the emitter, would prevent the electrodes from being in contact at ambient temperature. In this manner, spacings larger than 1.5-2.0 mils could be obtained. Spacings less than 1.5-2.0 mils can be reached by preheating the envelope before welding the emitter in place. On cool-down, the envelope-emitter structure would be pre-stressed, thus allowing the electrodes to remain in contact during operation until some minimum envelope temperature is attained.

5. PROGRAM FOR NEXT QUARTER

5.1 Variable-Parameter Test Vehicle

The experiments on the first set of electrode materials, rhenium-rhenium, will be completed and the results evaluated and compared to the performance from converter SN-101. A second set of materials will be selected and evaluated.

5.2 Secondary Experiments

The interelectrode spacing experiment will be concluded and the accuracy of calculating the interelectrode spacing via thermal expansion will be experimentally determined.

The ceramic-metal seal investigation may still be in progress, depending upon the seal lifetime. Metallurgical examination will conclude this study.

Collector heat transfer studies will be continued with an evaluation of the copper-molybdenum matrix to reduce the collector barrel ΔT (Ref. 1).

5.3 Converter Design

Converters SN-101, -102, and -103 will be designed, fabricated, and tested utilizing the data from the test vehicle, data from converter testing, and improved fabrication methods accruing from the program.

APPENDIX

DERIVATION OF COLLECTOR HEATING POWER

Plasma Electron Temperature in the Absence of a Collector Sheath

The plasma electron energy is the sum of the kinetic energy imparted to the electrons as they leave the emitter surface and the energy contributed by the emitter voltage fall. This is given by

$$\begin{aligned} E_{eject} + eV_{sheath} &= E_{plasma} \\ 2kT_{emitter} + eV_{sheath} &= E_{plasma} \end{aligned} \tag{1}$$

The controversy in this approach lies solely in the evaluation of the plasma energy. The mean electron energy, assuming a Maxwellian distribution, is defined by

$$\langle E \rangle = \frac{\int_0^\infty E dN_E}{\int_0^\infty dN_E} = \frac{\int_0^\infty 1/2MV^2 dN_v}{\int_0^\infty dN_v} = \frac{3}{2} kT \tag{2}$$

where dN_v is the Maxwellian distribution function for electrons with velocity between v and v + d. This is given by

$$dN_v = \left(\frac{4N}{\sqrt{\pi}}\right) \left(\frac{M}{2kT}\right)^{3/2} v^2 \exp\left(-\frac{MV^2}{2kT}\right) dv \tag{3}$$

The energy associated with the electrons having the average velocity is

$$E = 1/2M \langle v \rangle^2 = 1/2M \left[\frac{\int_0^\infty V dN_v}{\int_0^\infty dN_v} \right]^2 = \frac{4kT}{\pi} \qquad (4)$$

Whether Eq. 2 or 4 is the correct expression for the plasma electron energy is the question. Now, the random plasma current density is given by

$$\mathcal{J}_R = \frac{n_e \, e \, \langle v \rangle}{4}$$

Where n_e is the electron density; thus, Eq. 4 can be interpreted as the energy associated with the random electrons in the plasma. Since the random current densities exceed the drift current densities by greater than a factor of 10, it would seem appropriate to utilize Eq. 4 in evaluating the plasma electron temperature. Thus:

$$2kT_{emitter} + eV_{sheath} = \frac{4kT_{plasma}}{\pi} = 1.275kT_{plasma} \qquad (5)$$

The error in plasma temperature determination and thus collector energy input can be as much as 20 percent, depending on which plasma energy term (Eq. 2 or 4) is utilized.

Thus the heating power input to the collector is given by

$$P = \mathcal{J}_d A \left(\phi_c + \frac{2kT_{emitter}}{e} + V_{sheath} \right) = \mathcal{J}_d A \left(\phi_c + \frac{4kT_{plasma}}{\pi} \right) \qquad (6)$$

where

J_d = drift current density measured at the collector

A = collecting area

ϕ_c = collector work function

$T_{emitter}$ = emitter temperature

V_{sheath} = emitter sheath voltage

Plasma Electron Temperature with a Collector Sheath

In the case of a collector sheath, Eq. 6 is modified by the addition of a term representing the collector sheath voltage. That is,

$$P = J_d A \left(\phi_c + \frac{2kT_{emitter}}{e} + V_{sheath} \pm V_{collector}\right) \qquad (7)$$

where $V_{collector}$ is the height of the collector sheath and the sign is positive for an accelerating sheath and negative for a retarding sheath. There is a fine point in the evaluation of Eq. 7 since, when the collector sheath is retarding and the sign is negative, J_d will also decrease due to the loss of less energetic electrons. This will occur only in an "off" optimum mode of operation of a thermionic converter when the collector temperature is not high enough to emit sufficient electron density to equal the random plasma electrons impinging on the collector. In an optimized thermionic converter, the collector is analogous to an emitting probe that is matched to the plasma, i.e, the back emission from the collector is exactly equal to the positive x-directed random current. The positive x-direction is from the emitter toward the collector. In this instance there will be no sheath at the collector and a plasma-matched condition exists.

REFERENCES

1 First Quarterly Report, JPL Contract No. 951225, EOS Report 6952-Q-1

2 E. A. Baum and A. O. Jensen, Proceedings of the 15th Annual Power Sources Conference, May 1961

3 S. S. Kitrilakis, et al, Proceedings of the 24th Annual Physical Electronics Conference, Cambridge, March 1964

4 D. H. Pollock, Thermionic Specialist Conference, San Diego, October 1965